SUBMITTED TO APJ LETTERS
Preprint typeset using LaTeX style emulateapj v. 5/2/11

arXiv:1301.2330v1 [astro-ph.CO] 10 Jan 2013

THE VELOCITY FUNCTION OF DARK MATTER HALOS AT $R = 20$ KPC: REMARKABLY LITTLE EVOLUTION SINCE $z \approx 4$

SIMONE M. WEINMANN[1], MARIJN FRANX[1], PIETER VAN DOKKUM[2], RACHEL BEZANSON[2]

Submitted to ApJ Letters

ABSTRACT

We investigate the evolution in the dark matter halo circular velocity function, measured at a fixed physical radius of 20 kpc (v_{20}), which is likely to be a good proxy for galaxy circular velocity, in the Millennium-II simulation. We find that the v_{20} function evolves remarkably little since z $\approx$ 4. We analyze the histories of the main progenitors of halos, and we find that the dark matter distribution within the central 20 kpc of massive halos has been in place since early times. This provides evidence for the inside-out growth of haloes. The constancy of the central circular velocity of halos may offer a natural explanation for the observational finding that the galaxy circular velocity is an excellent predictor of various galaxy properties. Our results also indicate that we can expect a significant number of galaxies with high circular velocities already at $z = 4$ (more than one per $10^6 h^{-3}\mathrm{Mpc}^3$ with circular velocities in excess of 450 km s^{-1}, and more than one per $10^{4.5} h^{-3}\mathrm{Mpc}^3$ with circular velocities in excess of 350 km s^{-1}). Finally, adding baryonic mass and using a simple model for halo adiabatic contraction, we find remarkable agreement with the velocity dispersion functions inferred observationally by Bezanson et al. (2011) up to $z \approx 1$ and down to about 220 km s^{-1}.

Subject headings: galaxies: evolution — galaxies: kinematics and dynamics — galaxies: formation — galaxies: abundances — galaxies: halos

1. INTRODUCTION

Simulations of individual dark matter halos have provided evidence for the inside-out growth of halos in a ΛCDM cosmological model. These studies have shown that the inner few tens of kpc remain almost unchanged since high redshift both in massive halos (e.g. Loeb & Peebles 2003; Gao et al. 2004) and in halos expected to host Milky-Way sized galaxies (Wechsler et al. 2002; Diemand et al. 2007; Wang et al. 2011). From studying the mass-concentration relation of halos in cosmological simulations, it has become clear that the central density of haloes is correlated with their epoch of formation, which provides additional evidence for inside-out growth (Bullock et al. 2001a; Wechsler et al. 2002; Zhao et al. 2003).

The almost constant central densities of halos may have direct consequences for galaxy formation: At $z = 0$, the circular velocity at 10 kpc for dark matter halos has been found to be a good proxy for galaxy circular velocity and galaxy velocity dispersion (Loeb & Peebles 2003; Trujillo-Gomez et al. 2011). It is likely that this is also the case at higher redshift, and that central densities of halos can be used to predict galaxy circular velocities.

Motivated by these findings, we study the evolution of the circular velocity of dark matter halos at 20 kpc (hereafter v_{20}) in this work. We choose a radius of 20 kpc because galaxies in the nearby Universe are thought to have nearly isothermal mass profiles out to this scale. The scale is also small enough that we can expect structure to have formed very early (e.g. Diemand et al. 2007), and at the same time large enough that it is not completely dominated by baryonic processes.

We extend previous studies, which have focussed on individual halos, by studying the same quantity for a statistical sample of dark matter halos in the Millennium-II high-resolution cosmological simulation. Thus, we can for the first time explore the evolution of the small-scale circular velocity function of halos as a function of redshift.

weinmann@strw.leidenuniv.nl
[1] Leiden Observatory, Leiden University, P.O. Box 9513, 2300 RA Leiden, The Netherlands
[2] Department of Astronomy, Yale University, P.O. Box 208101, New Haven, CT 06520-8101, USA

2. DATA

We use the publicly available dark matter data from the Millennium-II simulation (hereafter MS-II, Boylan-Kolchin et al. 2009), which is contained in a box of side 137 Mpc and has a particle mass of $9.45 \cdot 10^6 \mathrm{M}_\odot$. According to eq. 20 in Power et al. (2003) the MS-II mass resolution is sufficient to resolve the circular velocity profile of halos down to 20 kpc and R_{max} for halos with masses above $10^{10}\mathrm{M}_\odot$. Particle data for this simulation is not available. Thus, we calculate v_{20} from R_{max}, R_{200} and v_{200} analytically, assuming a Navarro, Frenk & White (1997, NFW) profile:

$$\rho(R) = \frac{\rho_0}{(R/R_{\mathrm{s}})(1 + R/R_{\mathrm{s}})^2} \tag{1}$$

with the scale radius R_{s} and ρ_0 as the free parameters of the profile. The concentration of a NFW halo is defined as the ratio between scale radius and virial radius, $c = R_{\mathrm{s}}/R_{200}$. Given that the maximum circular velocity is reached at a radius $R_{\mathrm{max}} = 2.163 \cdot R_{\mathrm{s}}$ for a NFW halo, it follows that

$$c = 2.163 \cdot R_{200}/R_{\mathrm{max}}. \tag{2}$$

Integrating the NFW profile, the enclosed mass at radius R is given by

$$M(R) = 4\pi\rho_0 R_{\mathrm{s}}^3 \left[\ln(1 + cx) - \frac{cx}{1 + cx}\right] \tag{3}$$

with $x = R/R_{200}$. Given that $v_{\mathrm{circ}}(R) = \sqrt{\frac{GM(<R)}{R}}$ we can then calculate the circular velocity at 20 kpc using

$$v_{20} = v_{200} \cdot \left[\frac{1}{x} \cdot \frac{\ln(1 + cx) - \frac{cx}{1+cx}}{\ln(1 + c) - \frac{c}{1+c}}\right]^{0.5} \tag{4}$$

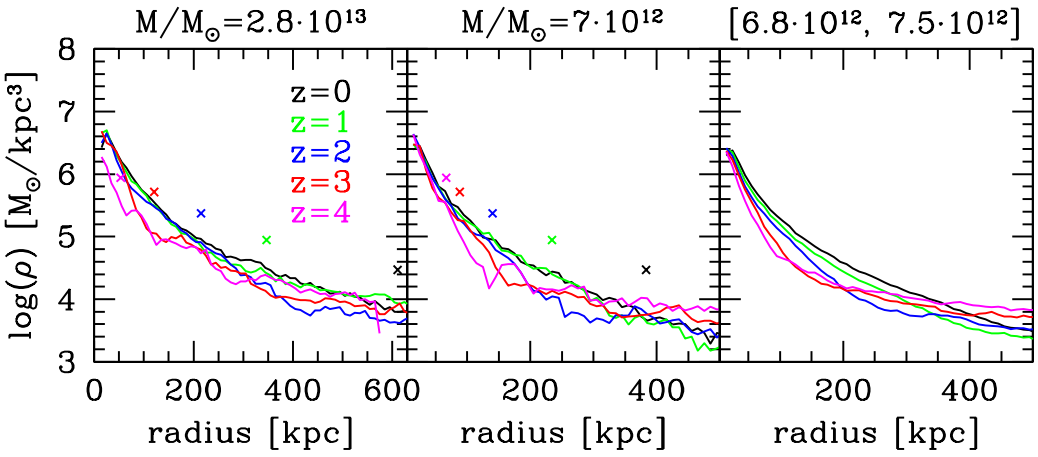

FIG. 1.— Evolution of the density profile of a randomly selected halo with a ($z = 0$) mass of $7 \cdot 10^{12} M_{\odot}$, and with a virial radius of 370 kpc (left) and with a mass of $2.8 \cdot 10^{13} M_{\odot}$ and 610 kpc (middle panel). Crosses show the location of the virial radius at each redshift. In the right panel, we show the average profile of 22 halos in a narrow bin in halo mass from $6.8 \cdot 10^{12} M_{\odot}$ to $7.5 \cdot 10^{12} M_{\odot}$, following the main progenitor history of halos. This figure shows that the density profile within $\approx$ 20–50 kpc undergoes only little evolution since $z \approx 4$.

with x=20 kpc/$R_{\rm vir}$. Klypin et al. (2001) show that NFW profiles fit numerically simulated profiles with a relative error of below about 10 % for radii larger than 1 % of the virial radius. The density at 20 kpc should thus be well described by a NFW profile.

For most of our analysis (with the exception of Fig. 1 and 4 where we only consider centrals), we use both central and type 1 satellite galaxies, only leaving out the 'orphan' galaxies without associated subhalos. For the satellite galaxies, we use $R_{\rm max}$ and v_{200} at the time of infall to calculate v_{20}, i.e. we assume that v_{20} stays unchanged after infall. This assumption seems reasonable, see Diemand et al. (2007).

We also make use of the lower-resolution Milli-Millennium simulation (hereafter Milli-MSI, Springel et al. 2005), which has a particle mass of $1.18 \cdot 10^9 {\rm M}_{\odot}$. For this simulation, individual particle data are available, which we use to calculate individual halo profiles, and to compare with the results from the MS-II simulation. Both the MS and MS-II simulations are based on a WMAP1 cosmology (Spergel et al. 2003).

3. RESULTS

3.1. *Particle data*

As a first step, we consider the dark matter profiles of central halos in the Milli-MSI simulation, calculated from particle data. In Fig. 1, left and middle panel, we show the evolution of the density profile up to $z = 4$ for two randomly selected halos. The halo shown in the left hand panel reaches a virial mass of $2.8 \cdot 10^{13} M_{\odot}$ and a virial radius of 610 kpc, the one in the middle panel a mass of $7 \cdot 10^{12} M_{\odot}$ and a virial radius of 370 kpc by $z = 0$. In the right panel of the same figure, we show the average profile of 22 halos in a narrow bin in stellar mass from $6.8 \cdot 10^{12} M_{\odot}$ to $7.5 \cdot 10^{12} M_{\odot}$. The central parts of haloes (inside 20–50 kpc) show only relatively little change, while there is significant growth on larger scales. We also show the location of the virial radius and virial density at different redshifts as crosses to indicate the significant evolution of those quantities. As a side note, absence of change in the inner part of the profile does not mean that the same dark matter particles stay in the inner region of the halo since $z \approx 4$ (e.g. Gao et al. 2004).

As a next step, we check the agreement between the statistical distribution of halo properties in the MS-II simulation with results from the Milli-MSI simulation. In Fig. 2, we show the halo mass, virial velocity, maximum circular velocity ($v_{\rm max}$) and v_{20} distribution for both simulations, with v_{20} calculated directly from the particle data for the Milli-MSI, and indirectly for the MS-II, at $z = 0$ and $z = 2$. In principle, the inner profile of halos can only be expected to be well resolved down to the limit given by Power et al. (2003). If we demand that less than 10 % of Milli-MSI halos fall below this limit, the resolution limit is about $v_{\rm vir}$=250 km s^{-1} at $z = 0$, and $v_{\rm vir}$=117 km s^{-1} at $z = 2$. We find that v_{20} for the two simulations is in reasonable agreement, although it appears to be slightly lower in the Milli-MSI simulation.

3.2. *Evolution in* v_{20}

In Fig. 3 we show the evolution of the halo mass function, virial velocity function, $v_{\rm max}$ function and v_{20} function. The halo mass function evolves dramatically over this time period. The virial velocity function and the $v_{\rm max}$ function also show significant evolution at the high mass end, indicating the formation of groups and clusters of galaxies. At intermediate values of $v_{\rm max} \approx 200$ km/s, little evolution is seen, in good agreement with results by Bullock et al. (2001b). Finally, very little evolution in the entire range of velocities is seen for the v_{20} function, which is well in place since $z = 4$. As we show below, this is likely connected to the inside-out growth of halos.

We then consider the main progenitor histories of halos in narrow halo mass bins at $z = 0$ in Fig. 4, averaging over 100–400 central halos in the three lower bins, and over 43 halos in the highest mass bin. In agreement with the previous figure, we can see circular velocities growing more slowly than halo mass, particularly at late times. Since $z = 1$, neither the average v_{20} nor the average $v_{\rm vir}$ has changed significantly in all mass bins. For the three higher bins, v_{20} has even stayed practically constant since $z = 2$. This figure is interesting since it allows us to directly read off the expected value of v_{20} for the main progenitor of a halo with a given final mass at $z = 0$. A halo with a mass of $10^{13} M_{\odot}$, which is expected to host a galaxy with a stellar mass of about $10^{11} M_{\odot}$ today (e.g. Moster et al. 2012) will have had $v_{20} \approx 250$ km s^{-1} since $z = 2$, and had reached $v_{20} \approx 160$ km s^{-1} already at $z = 6$. A halo with a mass of $10^{12} M_{\odot}$, which is expected to host a

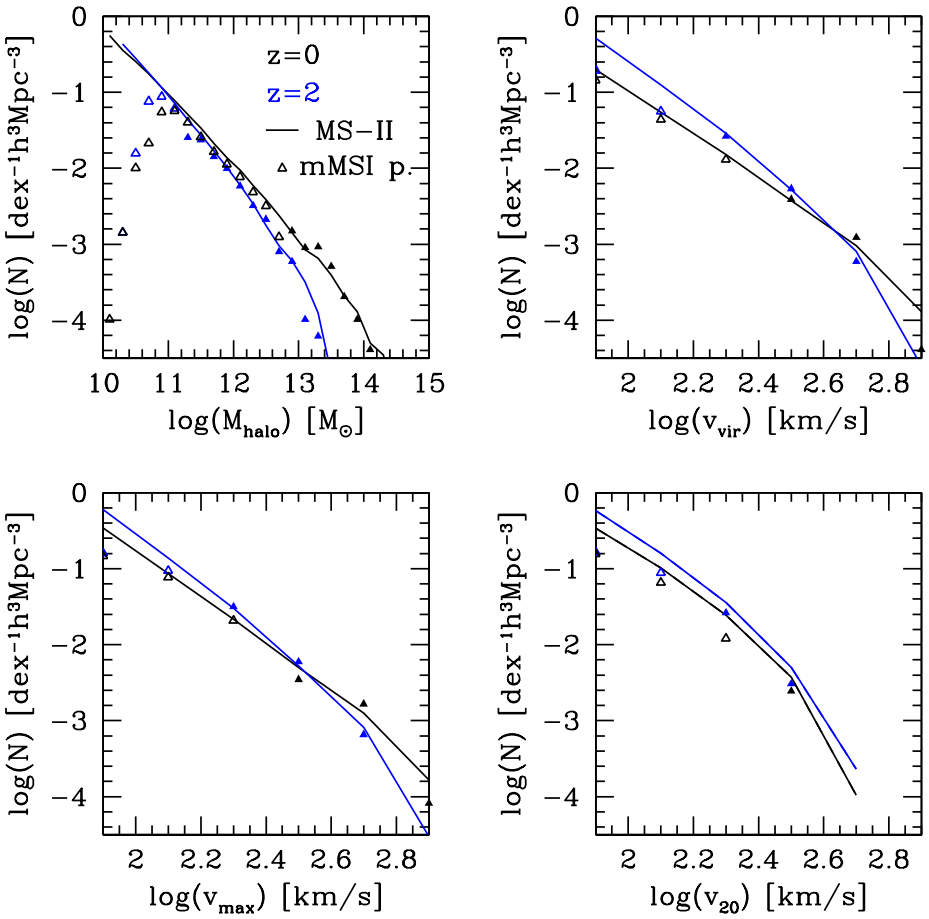

FIG. 2.— We compare results from MS-II (lines) to results from the Milli-MSI simulation particle data (symbols) down to the resolution limit. Filled symbols are results above the resolution limit according to Power et al. (2003), empty symbols below. The similarity of the results shows that velocity profiles of halos are reasonably well converged even below the resolution limit by Power et al. (2003).

galaxy with a stellar mass of about $2.5 \cdot 10^{10} M_\odot$ at $z = 0$ will have had $v_{20} \approx 180$ km s^{-1} since $z = 2$, and $v_{20} \approx 100$ km s^{-1} already at $z = 6$. From this we conclude that the main progenitors of today's massive galaxies will likely exhibit high circular velocity already at high redshifts.

3.3. *Comparison to observational results*

As a next step, we compare our findings to observational results of the galaxy velocity dispersion σ by Bezanson et al. (2011) and Bernardi et al. (2010), assuming $\sigma = v_{20}/\sqrt{2}$. Bernardi et al. (2010) calculate velocity dispersion functions from the SDSS using the spectroscopically measured quantity within the SDSS fiber. Bezanson et al. (2011) estimate the velocity dispersion of higher redshift galaxies using the stellar masses and radii, using a method calibrated on $z = 0$ data.

Assuming no halo contraction and no baryonic content, the agreement between the MS-II results and the observations is already encouraging (Fig. 5, top left panel). But of course, the presence of baryonic matter in the central regions of the halo, and the potential effect of halo contraction (Blumenthal et al. 1986; Trujillo-Gomez et al. 2011) should both serve to increase the central circular velocity dispersion.

We add baryonic mass according to

$$M_{20\mathrm{kpc}} = M_{20\mathrm{kpc,DM}} \cdot (1 - f_\mathrm{b}) + M_* \cdot (1 + f_\mathrm{gas}) \quad (5)$$

with $f_\mathrm{b} = 0.17$ the cosmic baryon fraction. We estimate M_* from the redshift-dependent relation between halo mass and stellar mass as given in Moster et al. (2012). For the cold gas fraction, $f_\mathrm{gas} = M_\mathrm{gas}/M_*$, we use the average $f_\mathrm{gas}(z, M_*)$ from the Guo et al. (2011) semi-analytical model. The result is shown in the top middle panel of Fig. 5. The difference to the dark matter-only model is small.

As a next step, we take into account the effect of adiabatic contraction (AC) using the Blumenthal et al. (1986) formula, iteratively solving the equation

$$r_\mathrm{i} \cdot M_\mathrm{tot}(r_\mathrm{i}) = r_\mathrm{f} \cdot [M_\mathrm{tot}(r_\mathrm{i}) \cdot (1 - f_b) + M_* \cdot (1 + f_\mathrm{gas})] \quad (6)$$

for r_i, with r_f =20 kpc. In case this formula results in halo expansion instead of contraction, we assume that the halo profile simply stays fixed. While the magnitude of the effect of adiabatic contraction, and even its existence, is still unclear and might differ for different galaxy types (e.g. Gnedin et al. 2004; Dutton et al. 2011), taking into account both the contribution of baryonic material and AC results in near perfect agreement with the Bezanson result (top right panel of Fig. 5) at the high velocity dispersion end. At lower velocity dispersions, the agreement breaks down. This is similar to the results obtained by Trujillo-Gomez et al. (2011) at $z = 0$.

The disagreement between our predictions and the results of Bezanson et al. (2011) at lower velocity dispersions may indicate that the simple relation between velocity dispersion and circular velocity breaks down for disky galaxies with a small bulge component. In addition, the estimates for velocity dispersions used by Bezanson et al. (2011) might become

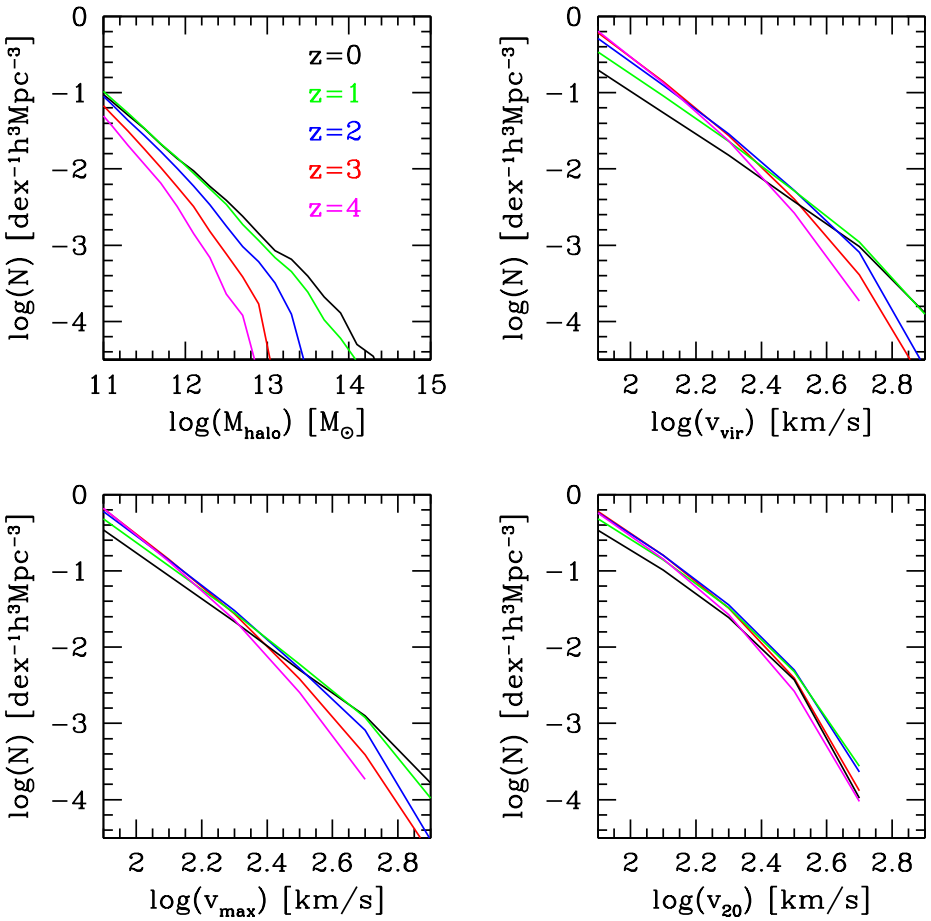

FIG. 3.— Evolution of the halo mass, virial velocity, $v_{\rm max}$ and v_{20} functions at different redshifts. While the halo mass function undergoes substantial growth at all masses, the $v_{\rm max}$ and virial velocity function only grow at the high velocity end, and actually decrease at the low velocity end. The v_{20} function undergoes remarkably little change since $z = 4$.

progressively uncertain for lower-mass galaxies, due to the increasing contribution of face-on disks and the higher gas and dark matter content of low-mass galaxies (but see Taylor et al. 2010 who find that the method works well down to 100 km s^{-1} at $z = 0$). The fact that the agreement improves towards lower redshifts might indicate that velocity dispersions are particularly difficult to estimate for highly star-forming, gas-rich galaxies. Bezanson et al. (2012) show that the σ below which more than 50 % of all galaxies are star-forming decreases towards lower redshift, a signature of downsizing. In all, the cause of the disagreement at low velocity dispersions is not entirely clear, but the agreement is excellent in the high-mass regime where elliptical, passive and probably gas-free galaxies dominate. We note that previous studies have found strong and puzzling disagreement between observations and model predictions at even lower velocity dispersions, below 100 km s^{-1} (Zavala et al. 2009), with many more low-velocity dispersion galaxies predicted by models. One potential explanation is that dark matter halos are strongly influenced by baryonic processes in this regime (Sawala et al. 2012).

Finally, in the bottom row of Fig. 5, we show the cumulative distributions of v_{20} and $v_{\rm max}$. In the bottom left panel, we show v_{20} calculated from dark matter alone, in the middle panel v_{20} including the effect of baryons and AC. These two figures can be used to read off predictions about the number density of galaxies with v_{20} above a certain limit. In the bottom right panel of the same figure, we compare our cumulative $v_{\rm max}$ function to the analytic fit of Klypin et al. (2011) based on the Bolshoi simulation, which uses a WMAP7 cosmology (Komatsu et al. 2011). The agreement is reasonable given the different cosmology, with the MS-II simulation predicting more high mass haloes, as expected. Similar results have been obtained from a comparison between WMAP1 and WMAP7 velocity functions in Guo et al. (2013).

4. SUMMARY AND DISCUSSION

Using the MS-II simulation, and particle data from the Milli-MSI, we have investigated the evolution of the circular velocity of dark matter halos at 20 kpc, v_{20}. Our main results are the following:

- For halos with mass $\log(M/M_\odot) > 12$, the mass profile within 20–50 kpc changes only little since about $z \approx 4$, despite significant growth in halo mass. Following the main progenitor history, we find almost no evolution in v_{20} over this time period.

- As a consequence, the v_{20} function of halos is almost in place at $z = 4$.

- By using v_{20} as a proxy for the circular velocity of the galaxy, we can reproduce observations of the velocity dispersion of massive galaxies by Bezanson et al.

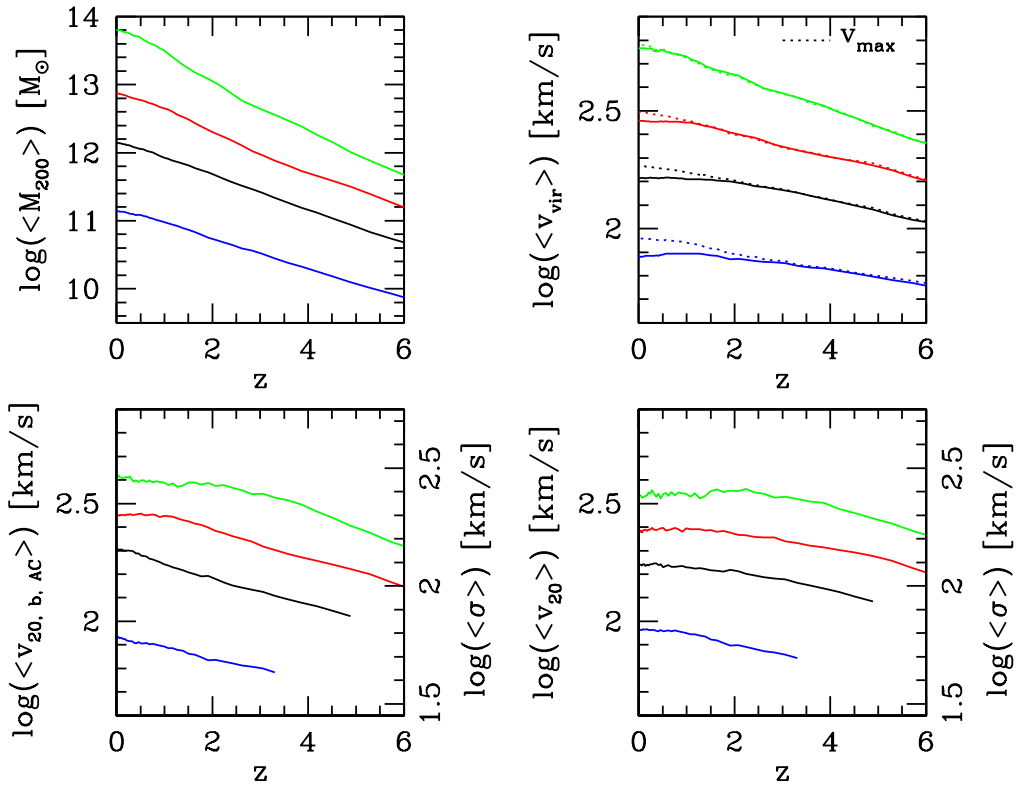

FIG. 4.— Evolution of the average halo mass, virial velocity and $v_{\rm max}$, and v_{20}, for the main progenitors of halos in four bins of M_{200} at $z = 0$. The top two panels and the bottom right are based on dark matter results only, the bottom left panel shows v_{20} after correction for baryons and AC. Results for v_{20} are only shown as long as $v_{20} < v_{\rm max}$. The right axis of the bottom two panels show rescaled results for $\sigma = v_{20}/\sqrt{2}$. Confirming results from Fig. 3, v_{20} undergoes only little change since $z \approx 2 - 4$, depending on the halo mass bin.

(2011) remarkably well. The agreement is nearly perfect if we take into account the baryon content of halos inferred from abundance matching, and by considering the Blumenthal et al. (1986) prescription for adiabatic contraction. The observations of Bezanson et al. (2011) are thus in excellent agreement with basic ΛCDM predictions on the evolution of structure in the Universe.

These results have interesting implications. First of all, we expect a significant number of galaxies (more than one per $10^6 h^{-3}{\rm Mpc}^3$) with circular velocities in excess of 450 km s^{-1} already at $z = 4$. We also expect more than one per $10^{4.5} h^{-3}{\rm Mpc}^3$ with circular velocities in excess of 350 km s^{-1} up to $z = 4$. Our results thus predict that high line widths should be found in high redshift galaxies with the Atacama Large Milimeter/Submilimeter Array (ALMA).

Second, we infer that the main progenitors of today's most massive galaxies must have had high circular velocities already at high redshifts. This means that the circular velocity can be used to link massive galaxies with their progenitors and descendants. It also helps to understand the fact that high redshift galaxies have higher circular velocity at given dynamical mass than their local counterparts. Recently, van de Sande et al. (2011) have measured a velocity dispersion of ≈ 300 km s^{-1} in a galaxy at $z = 1.8$ with $M_*/M_\odot \approx 1.7 \cdot 10^{11}$, corresponding to a very high velocity dispersion for its dynamical mass compared to today's galaxies. As seen in Fig. 4, the galaxy will continue to grow in halo mass (and probably also in stellar mass) to $z = 0$, but its circular velocity has likely almost reached its final value by $z \approx 2$. An even more extreme example is the extremely high velocity-disperson galaxy (510 km s^{-1}) discovered by van Dokkum et al. (2009).

Finally, our result might offer an explanation for a puzzling recent observational result. Wake et al. (2012a, b) have found that galaxy circular velocities are an excellent predictor not only of the clustering properties of galaxies, but also of galaxy colours, specific star formation rates and ages, being superior to galaxy stellar mass or surface mass density. As we have shown in this work, the galaxy circular velocity, unlike the galaxy stellar mass, stays almost constant since early times. It thus might constitute a galaxy property that is more fundamental than stellar mass, retaining some memory of the initial conditions of the galaxy's formation.

We thank the referee for helpful comments, which improved the paper. We acknowledge funding from ERC grant HIGHZ no. 227749. SQL databases containing the simulation data from Millennium and Millennium-II simulations are publicly released at `http://www.mpa-garching.mpg.de/millennium`. The Millennium site was created as part of the activities of the German Astrophysical Virtual Observatory. Tables for the velocity function of halos as shown in this paper can be found at `http://www.strw.leidenuniv.nl/galaxyevolution/v20function/`.

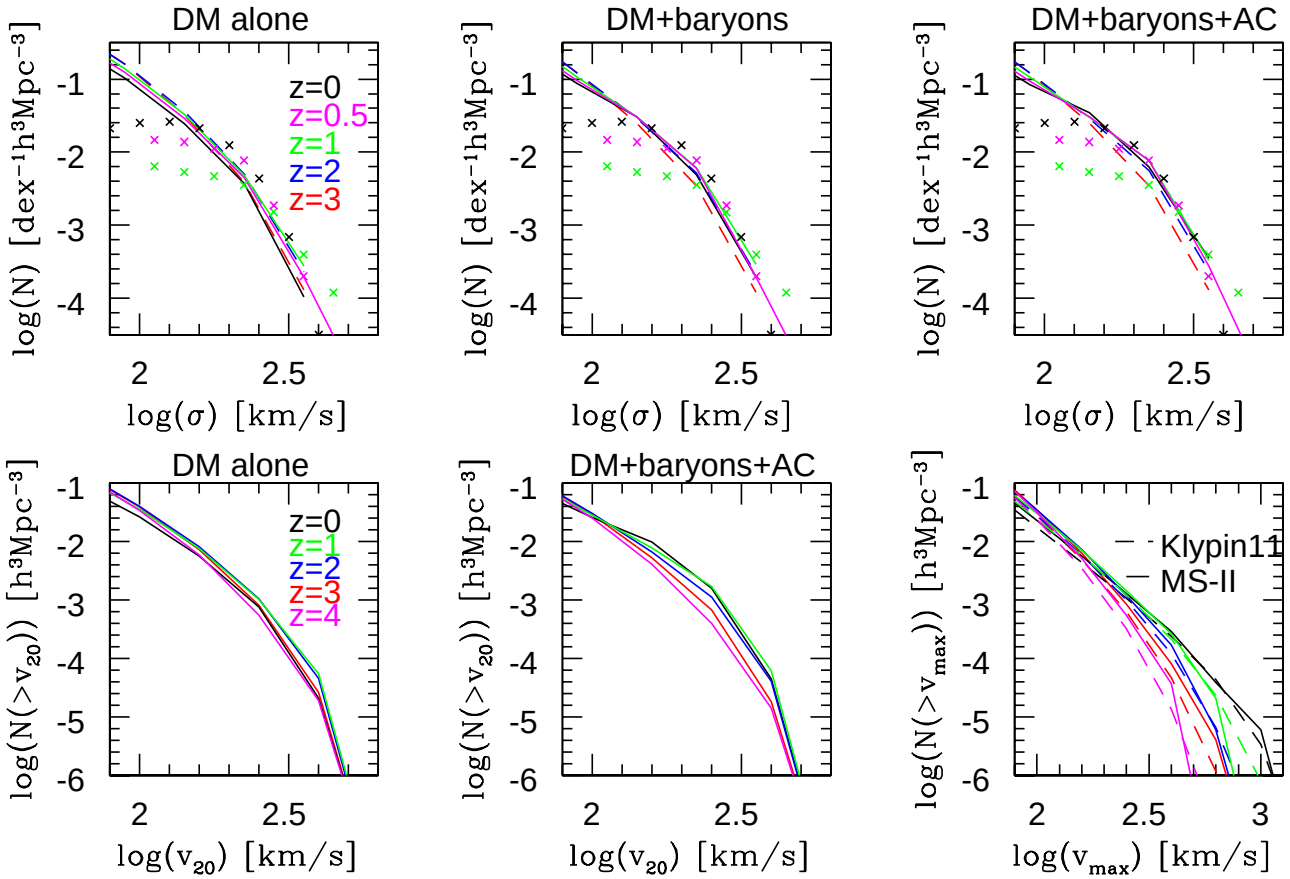

FIG. 5.— Top panels: Comparison of σ at 20 kpc (i.e. $v_{20}/\sqrt{2}$) to results by Bezanson et al. at $z = 0.45$ and $z = 1.05$, and Bernardi et al. (2010) at $z = 0$ (crosses). We also show predictions for $z = 2$ and $z = 3$ as dashed lines. Results are shown for dark matter alone (top left panel), dark matter and baryons (top middle panel), and dark matter, baryons and AC (top right panel). Agreement between theoretical predictions and the Bezanson et al. (2011) results are excellent for the high mass end of the velocity dispersion function. Bottom panels: Cumulative functions. Bottom left panel: v_{20}-function, only taking into account dark matter. Middle panel: Same like left hand panel, but with the contribution of baryons and AC added. Right hand panel: Cumulative $v_{\rm max}$-function, compared to the analytical fits of Klypin et al. (2011) based on the Bolshoi simulation.

REFERENCES

Bernardi M., Shankar F., Hyde J.B., Mei S., Marulli F., Sheth R.K., 2010, MNRAS, 404, 2087
Bezanson R. et al., 2011, ApJ, 737, 31
Bezanson R., van Dokkum P, Franx M., 2012, ApJ, 760, 62
Blumenthal G.R., Faber S.M., Flores R., Primack J.R., 1986, ApJ, 301, 27
Boylan-Kolchin M., Springel V., White S.D.M., Jenkins A., Lemson G., 2009, MNRAS, 398, 1150
Bullock J.S. et al., 2001a, MNRAS, 321, 559
Bullock J.S., Dekel A., Kolatt T.S., Primack J.R., Somerville R.S., 2001b, ApJ, 550, 21
Diemand J., Kuhlen M., Madau P., 2007, ApJ, 667, 859
Dutton A.A., 2011, MNRAS, 416, 322
Gao L., Loeb A., Peebles P.J.E., White S.D.M, Jenkins A., 2004, ApJ, 614, 17
Gnedin O.Y., Kravtsov A.V., Klypin A.A., Nagai D., 2004, ApJ, 616, 16
Guo Q. et al., 2011, MNRAS, 213, 101
Guo Q., White S., Angulo R.E., Henriques B., Lemson G., Boylan-Kolchin M., Thomas P., Short S., 2013, 428, 1351
Klypin A., Kravtsov A.V., Bullock J.S., Primack J.R., 2001, ApJ, 554, 903
Klypin A.A., Trujillo-Gomez S., Primack J., 2011, ApJ, 740, 102
Komatsu et al., 2009, ApJS, 180, 330
Loeb A., Peebles P.J.E., 2003, ApJ, 589, 29
Moster B.P., Naab T., White S.D.M., 2012, preprint, arXiv:1205.5807
Navarro J.F., Frenk C.S., White S.D.M., 1997, ApJ, 490, 493
Power C., Navarro J.F., Jenkins A., Frenk C.S., White S.D.M., Springel V., Stadel J., Quinn T., 2003, MNRAS, 228, 14
Sawala T. et al., preprint, 2012, arXiv:1206:6496
Spergel et al., 2003, ApJS, 148, 175
Springel V. et al., 2005, Nature, 435, 629
Taylor E.N., Franx M., Brinchmann J., van der Wel A., van Dokkum P.G., 2010, ApJ, 722, 1
Trujillo-Gomez S., Klypin A., Primack J., Romanowski A.J., 2011, ApJ, 742, 16
van Dokkum P.G., Kriek M., Franx M., 2009, Nature, 460, 717
van de Sande J. et al., 2011, ApJ, 736, 9
Wechsler R.H., Bullock J.S., Primack J.R., Kravtsov A.V., Dekel A., 2002, ApJ, 568, 52
Wake D.A., van Dokkum P.G., Franx M., 2012a, ApJ, 751, 44
Wake D.A., Franx M., van Dokkum P.G., 2012b, preprint, arXiv:1201.1913
Wang J. et al., 2011, MNRAS, 413, 1373
Zavala J., Jing Y.P., Faltenbacher A., Yepes G., Hoffman Y., Gottlöber S., Catinella B., 2009, ApJ, 700, 1779
Zhao D.H., Jing Y.P., Mo H.J., Börner G., 2003, ApJ, 597, L9